ISSN 1330-3651 (Print), ISSN 1848-6339 (Online)
https://doi.org/10.17559/TV-20160203000313
Original scientific papers

Mechanical Analysis of Roof Subsidence Based on Rheological Properties of Solid Backfill Materials

Meng LI, Jixiong ZHANG, Rui GAO

Abstract: To study the influence of the rheological properties of backfill materials on strata movement during solid backfill mining, Poyting-Thomson model was selected as the rheological model for the backfill materials based on their experimentally derived rheological properties. By regarding the roof as a thin elastic plate, a rheological mechanical model of the roof when using solid backfill mining, was established. According to the elastic-viscoelastic correspondence principle, the deflection of the roof at different times was obtained by use of the energy method. By taking the 7203W backfill mining panel of a coalmine in Zhaizhen town as an example, the subsidence of the roof over time was calculated. Results showed that the maximum subsidence was 205 mm, which was close to that measured in situ. Meanwhile, the observation of boreholes drilled into the roof evinced its integrity. Therefore, these results can provide a theoretical basis for predicting strata movement and surface subsidence during solid backfill mining.

Keywords: backfill materials; rheological properties; roof subsidence; solid backfill mining

1 INTRODUCTION

Solid backfill mining is a green mining method used to overcome the difficulties in coal mining including unexploited coal under railways, water bodies and buildings, and the gangue piles on the surface [1, 2]. This method directly fills solid wastes including gangue, aeolian sand, slag, etc. into mined-out areas so as to replace unexploited coal and protect surface buildings and the environment. After coal has been mined, backfill materials are filled into the mined-out area and serve as permanent carrier structures to support overlying strata [3]. In this way, slow subsidence occurs in the overlying strata so that their movement and surface subsidence can be controlled [4]. The characteristics of strata movement during solid backfill mining differ from those in traditional caving methods [5÷7]. The characteristics of strata movement when using solid backfill mining have been investigated by theoretical work and simulations as well as field measurement. For example, Miao [8] proposed an equivalent mining height theory for backfill mining. Based on the equivalent mining height, a mining pressure model for the strata movement when using solid backfill mining, was established. Zhang et al. [9] established a mechanical model of the key strata among the overburden in a fully-mechanised panel. Afterwards, they analysed the characteristics of the bending deformation thereof by using the theory of beams on elastic foundations. Li et al. [10] established a mechanical model of an elastic thin plate within the overlying strata when using solid backfill mining and derived a deflection equation for the roof using the principle of virtual work. Huang et al. [11] tested the time-dependent properties of fly-ash backfill materials, and a PTH model was used as the rheological model for backfill materials. All of the aforementioned research can give theoretical guidance for the deformation characteristics of the overlying strata at a coal panel; however, there are some limitations as none of them took the effect of time on strata movement into consideration. When backfill materials are placed into mined-out areas, rheological effects manifest themselves over time. Therefore, it is important to study the influence of the rheological properties of backfill materials on strata movement.

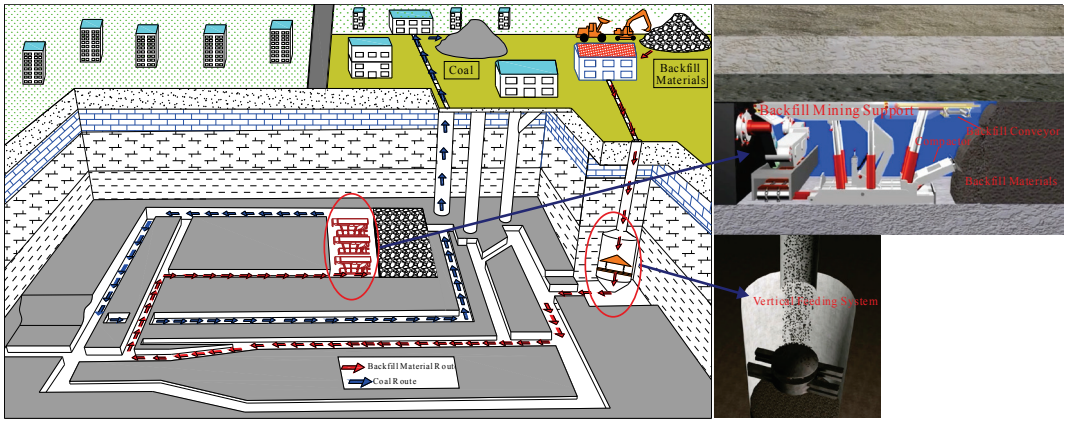

Figure 1 Basic principle of solid backfill mining

Therefore, based on rheological experiments, this paper established a rheological mechanical model for the coalmine roof when using solid backfill mining by considering the rheological properties of backfill materials. Then, based on this model, the deflection of the roof at different times was calculated. Taking the 7203W

backfill mining panel of Zhaizhen Coal Mine as an example, the strata movement under different rheological conditions in the backfill material, when using solid backfill mining, was studied. All these aimed to provide a reference for the precise prediction of strata movement and surface subsidence when using solid backfill mining.

2 BASIC PRINCIPLE OF SOLID BACKFILL MINING

As shown in Fig. 1, gangue, loess, slag, aeolian sand, fly ash, etc., as backfill materials, were conveyed to an underground storage silo by a vertical feeding system. Then the backfill materials were transported to the backfill mining face [12]. After that the backfill materials were backfilled into the goaf by the backfill conveyor hanging on the back top beam of the backfill mining hydraulic support. Finally, the compactor behind the backfill mining hydraulic support was used to compact the backfill materials to ensure better support of the roof, reduce overlying strata movement, and control surface subsidence [2, 13].

3 RHEOLOGICAL PROPERTIES OF BACKFILL MATERIALS

3.1 Rheological Experiments

Gangues used as backfill materials were collected from the solid backfill mining panel. In the collection process, the artificial destruction of the backfill material needed to be avoided as much as possible. Then, the materials were sieved using a standard stone screen with a maximum square mesh aperture of 50 mm. The obtained grading curve is shown in Fig. 2.

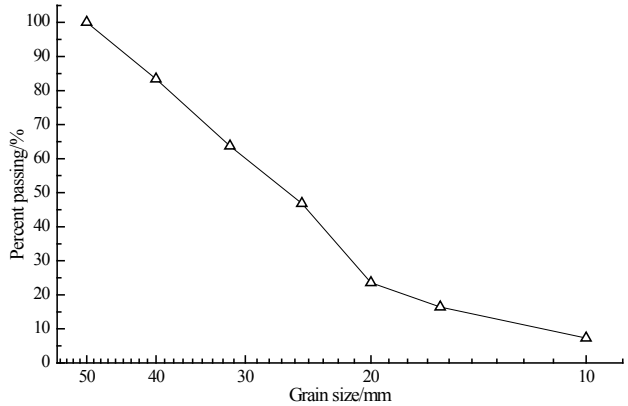

Figure 2 Grading curve of backfill material

The experimental system used to measure the rheological properties of the backfill material included a loading device and a compacting device, as shown in Fig. 3. The YAS-5000 electro-hydraulic servo pressure tester (Changchun Kexin Experimental Equipment Co., Ltd), China) was used as the loading device. With a maximum axial force of 5,000 kN, this machine can provide a measure-control range of up to 250 mm stroke. A steel cylinder (internal and external diameters of 125 mm and 137 mm, and a height of 305 mm) was used to contain the samples during compaction. The loading piston (radius 124 mm, thickness 40 mm) was used to apply both compactive effort and load (see Fig. 4).

A uniaxial compression test with lateral confinement under single-stage loading was performed. According to the grading curve in Fig. 2, five groups of backfill material samples were prepared. Then, the rheological properties of each sample were tested under five applied pressures: 2 MPa, 5 MPa, 10 MPa, 15 MPa, and 20 MPa.

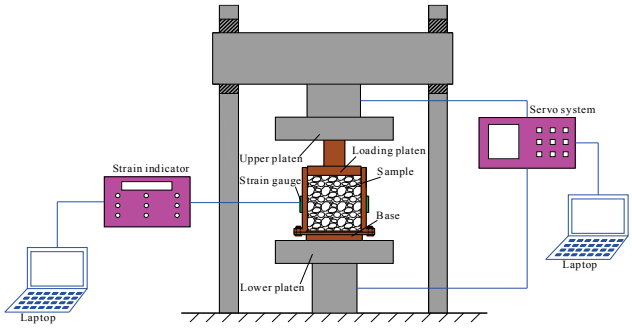

Figure 3 Experimental system for rheological properties

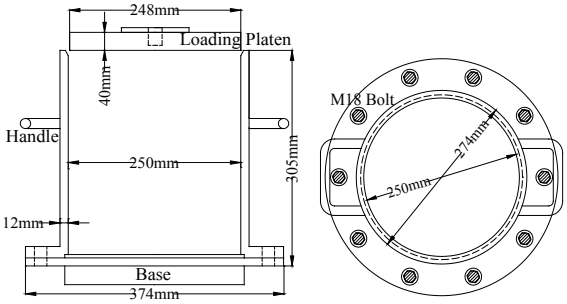

(a) Front elevation (b) Cross-section

Figure 4 Dimensions of the compacting device

3.2 Rheological Model

Based on the acquired experimental data, the axial strain-time curves of these samples under different stress states were drawn (see Fig. 5).

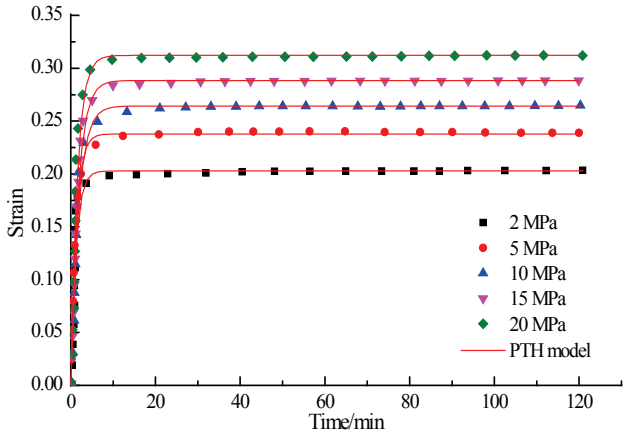

Figure 5 Rheological curves of backfill materials under different stress

As shown in Fig. 5, the rheological curves of backfill materials under different stress states presented similar variations: an obvious initial rheology and that in the later stages. Initially, the rheology was rapidly developed; these rheological curves exhibited gradually reducing slopes and tended to develop into a stable rheology in the later stages. Thereafter, the creep gradually slowed down and tended to a stable state. The slopes of these plots became zero, that is to say, except for the declining stage

and stable stage, there was no accelerated creep. In addition, under different axial stresses, there were different creep deformations for gangue samples. This suggested that pressure had a significant influence on the deformation of gangue samples: the larger the axial stress, the larger the corresponding deformation. Therefore, according to the actual rheological properties of these backfill materials, Poyting-Thomson (PTH) model was used as the rheological model for them (see Fig. 6).

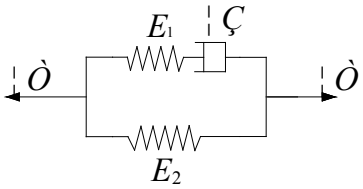

Figure 6 PTH rheological model

The constitutive equation for this PTH model is as follows:

$$\dot{\sigma}+\frac{E_1}{\eta}\sigma=(E_1+E_2)\dot{\varepsilon}+\frac{E_1E_2}{\eta}\varepsilon, \tag{1}$$

where, E_1 and E_2 are the stiffness coefficients and η is the viscosity coefficient.

When stress σ_0 is constant, then the rheological equation becomes:

$$\varepsilon=\frac{\sigma_0}{E_2}(1-\frac{E_1}{E_1+E_2}e^{-\frac{E_1E_2}{(E_1+E_2)\eta}t}), \tag{2}$$

Based on their nonlinear best-fit (see Fig. 5), the rheological model of PTH predicted the results of subsequent rheological experiments. This indicated that the established rheological model was reasonable.

4 RHEOLOGICAL MECHANICAL MODEL

4.1 Model Establishment

Solid backfill mining replaces raw coal through backfill bodies. After coal is mined, backfill bodies are used to occupy the mined-out area and substitute raw coal to support the overlying strata. Therefore, it can significantly change the characteristics of strata movement: it can prevent the strata from being fractured so as to avoid caving zones being formed; moreover, the height of the fractured zones caused by mining decreases, which can relieve surface subsidence to a significant extent. The structure of overlying strata shows greater integrity. When using solid backfill mining, it is therefore more suitable to regard the overlying key stratum as an elastic thin plate based on the hypothesis of a continuous medium [14]. Fig. 7 shows the characteristics of strata movement when using solid backfill mining.

Solid backfill mining was used to eliminate caving zones to further avoid roof fracture. Therefore, the roof could be regarded as an integrated elastomer. The solid backfill mining panel was generally 80 to 150 m long and the roof was 3 to 20 m thick [10]. If the ratio of thickness to width of the roof meets the requirements of an elastic thin plate, it could be regarded as such. While, based on rheological experiments, the backfill materials fitted the PTH viscoelastic model under the effects of long-term load from overlying strata. Therefore, the roof could be treated as a thin plate whose four edges were clamped. Moreover, its upper part was subjected to load from the overlying strata and its lower part was supported by a viscoelastic foundation.

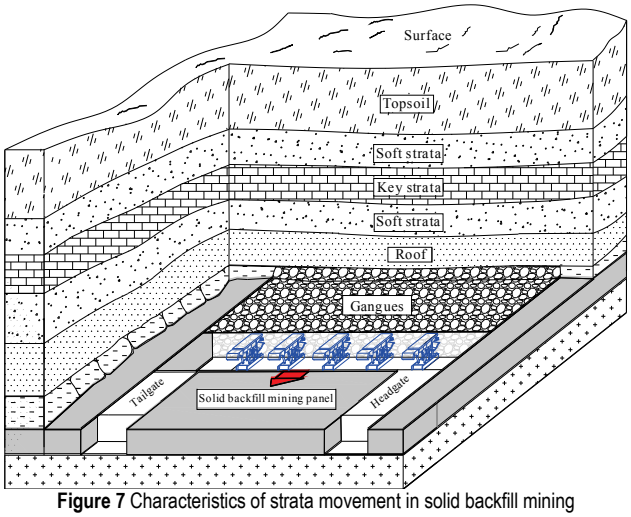

Figure 7 Characteristics of strata movement in solid backfill mining

Taking the internal corner o of the plate as the origin, a coordinate system was established with the advancing direction of the panel as the x-axis and the length direction of the panel as the y-axis. Therein, b represents the length of the panel; a is the advance length; q represents the imposed load from any overlying strata; E_1 and E_2 denote the stiffness coefficients of the viscoelastic foundation, while η is the viscosity coefficient. The established rheological mechanical model of roof is shown in Fig. 8.

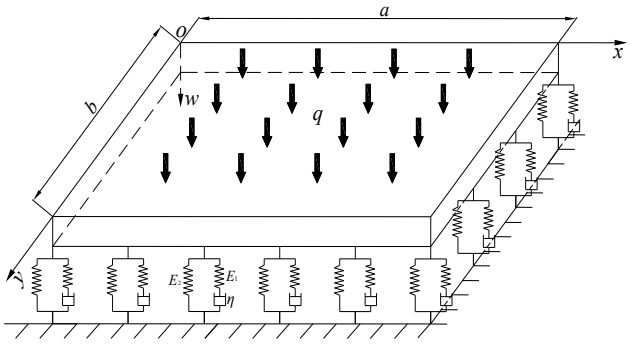

Figure 8 Rheological mechanical model

4.2 Model Solution

The deflection of a roof with four edges fixed is as follows:

$$w=a_0(1-\cos\frac{2\pi x}{a})(1-\cos\frac{2\pi y}{b}), \tag{3}$$

Given that the system comprised the roof and a viscoelastic foundation, the total potential energy Π of the system consisted of deformation energy U and exogenous force energy V of the roof.

The bending deformation energy of the roof is

$$U = \frac{1}{2}D\iint(\frac{\partial^2 w}{\partial^2 x}+\frac{\partial^2 w}{\partial^2 y})^2 \mathrm{d}x\mathrm{d}y = 2D\pi^4 aba_0^2(\frac{3}{a^4}+\frac{2}{a^2b^2}+\frac{3}{b^4}), \quad (4)$$

where, D represents the flexural rigidity of the thin plate.

The exogenous force energy of the whole system is comprised of the potential energy V_1 resulting from the overlying strata load and the potential energy V_2 arising from the reaction of the viscoelastic foundation.

$$\begin{cases} V_1 = -a_0\int_0^a\int_0^b q[(1-\cos\frac{2\pi x}{a})(1-\cos\frac{2\pi y}{b})]dxdy \\ \quad = -a_0 qab \\ V_2 = \frac{1}{2}ka_0^2\int_0^a\int_0^b[(1-\cos\frac{2\pi x}{a})(1-\cos\frac{2\pi y}{b})]^2 dxdy \\ \quad = ka_0^2\frac{9ab}{8} \end{cases}, \quad (5)$$

Then, the total potential energy Π of the whole system is

$$\prod = 2D\pi^4 aba_0^2(\frac{3}{a^4}+\frac{2}{a^2b^2}+\frac{3}{b^4})-(a_0 qab - ka_0^2\frac{9ab}{8}), \quad (6)$$

According to the principle of minimum potential energy:

$$a_0 = \frac{q}{4D\pi^4(\frac{3}{a^4}+\frac{2}{a^2b^2}+\frac{3}{b^4})+\frac{9k}{4}}, \quad (7)$$

Substituting Eq. (7) into Eq. (3) gives the deflection of the roof:

$$w = \frac{q(1-\cos\frac{2\pi x}{a})(1-\cos\frac{2\pi y}{b})}{4D\pi^4(\frac{3}{a^4}+\frac{2}{a^2b^2}+\frac{3}{b^4})+\frac{9k}{4}}, \quad (8)$$

Based on the Winkler hypothesis, the reaction of the foundation to the roof is as follows:

$$p(x,y,t) = kw(x,y,t), \quad (9)$$

Combining Eqs. (1) and (9) gives:

$$\dot{p}+\frac{E_1}{\eta}p = (E_1+E_2)\dot{w}+\frac{E_1E_2}{\eta}w, \quad (10)$$

The Laplace transform of Eq. (10) gives:

$$s\overline{p}+\frac{E_1}{\eta}\overline{p} = (E_1+E_2)\mathrm{s}\,\overline{w}+\frac{E_1E_2}{\eta}\overline{w}, \quad (11)$$

Algebraic manipulation of Eq. (11) gives:

$$sk(s) = \frac{\overline{p}}{\overline{w}} = \frac{\eta s(E_1+E_2)+E_1E_2}{\eta s+E_1}, \quad (12)$$

The Laplace transform of Eq. (8) gives:

$$\overline{w}(x,y,s) = \frac{q(1-\cos\frac{2\pi x}{a})(1-\cos\frac{2\pi y}{b})}{(4D\pi^4(\frac{3}{a^4}+\frac{2}{a^2b^2}+\frac{3}{b^4})+\frac{9k}{4})s}, \quad (13)$$

Based on the elastic-viscoelastic correspondence principle [15, 16], and considering the foundation as a viscoelastic body where k is time-dependent, $sk(s)$ can be used to replace k in Eq. (13). Then by substituting Eq. (12) into Eq. (13):

$$\overline{w}(x,y,s) = \frac{q(1-\cos\frac{2\pi x}{a})(1-\cos\frac{2\pi y}{b})}{(4D\pi^4(\frac{3}{a^4}+\frac{2}{a^2b^2}+\frac{3}{b^4})+\frac{9}{4}\frac{\eta s(E_1+E_2)+E_1E_2}{\eta s+E_1})s}, \quad (14)$$

Back analysis of Eq. (14) gave the deflection of the roof on a viscoelastic foundation. Before evaluating the Laplace transform of Eq. (14), the following parameters were set:

$$\begin{aligned} A &= \frac{4}{9}q(1-\cos\frac{2\pi x}{a})(1-\cos\frac{2\pi y}{b}) \\ B &= \frac{16}{9}D\pi^4(\frac{3}{a^4}+\frac{2}{a^2b^2}+\frac{3}{b^4}) \\ C &= \frac{BE_1+E_1E_2}{\eta(B+E_1+E_2)}, \end{aligned} \quad (15)$$

Substituting Eq. (15) into Eq. (14) gives

$$\overline{w}(x,y,s) = A(\frac{\frac{E_1}{\eta(B+E_1+E_2)}}{s(s+C)}+\frac{\frac{1}{B+E_1+E_2}}{s+C}), \quad (16)$$

After taking the Laplace inverse transform of Eq. (16), the time-dependent deflection of the roof on its viscoelastic foundation is given by:

$$w(x,y,t) = A(\frac{E_1}{\eta C(B+E_1+E_2)}(1-e^{-Ct})+\frac{1}{B+E_1+E_2}e^{-Ct}), \quad (17)$$

5 CASE STUDY

For solid backfill materials like gangue, slag, aeolian sand and fly ash, the rheological mechanical model can be used to obtain the effect of time on strata movement. In order to validate the feasibility of research results, a case study was proposed below.

The tested site was located at the 7203W backfill mining panel in the No. 2 Zhaizhen Coal Mine. The corresponding surface and underground elevations were +177.1 m to +181.2 m, and −340 m to −384.6 m, respectively. With strike length a and inclination b of 286 m and 92.8 m respectively, the average burial depth H of

the coal seam was 540 m. The mining height M was 2.7 m and there were about 93,800 tonnes of recoverable reserves. With an elastic modulus E of 12 GPa and a Poisson's ratio u of 0.28, the roof was composed of sandstones with 11.8 m thickness (h). The surface corresponding to the panel was covered with closely-spaced buildings. The gangue samples were collected to test the rheological properties. And gangues with stiffness coefficients E_1 and E_2 of 5 GPa and 0.07 GPa, and a viscosity coefficient η of 30 GPa·h were used as backfill materials in the mined-out area by fitting the rheological curve with PTH model.

By substituting the above parameters into Eq. (17), the subsidence curve of the central position (143, 46.4) of the roof over with time was calculated (see Fig. 9).

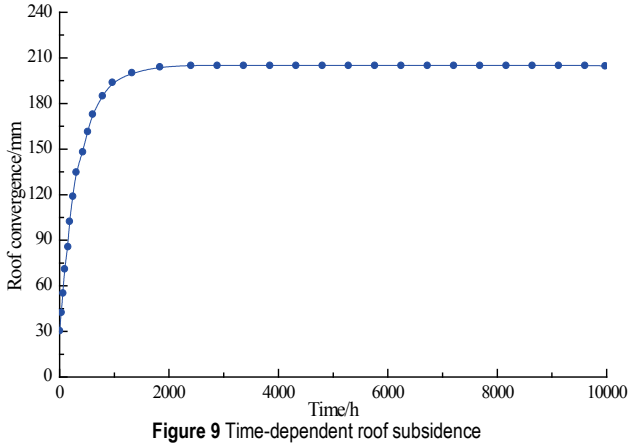

Figure 9 Time-dependent roof subsidence

Fig. 9 shows that the roof gradually subsided under the support of the backfill materials. The instantaneous subsidence of the central position in the roof was about 30 mm. Over time, the backfill materials underwent creep and the roof gradually subsided. After several months of slow subsidence, the roof subsidence approached 205 mm at 5,000 h, the subsidence of the roof at different positions was as shown in Fig. 10.

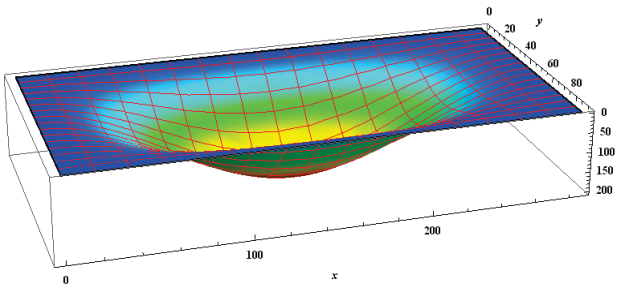

Figure 10 Three-dimensional roof subsidence

Fig. 9 shows that the maximum subsidence of the roof was 205 mm, which occurred in the centre of the panel. The ratio of maximum deflection to roof thickness (2.7 m) was 0.075 (i.e. less than 0.2). Accordingly, it satisfied the minor deflection bending limit for this roof. During the mining of the 7203W backfill mining panel, the maximum roof subsidence in the mined-out area, measured by dynamic displacement meter, was 201 mm, which was similar to that measured in situ (Fig. 11). Meanwhile, by drilling boreholes on the roof in the mined-out area behind the panel, the development of fissures in the roof was observed and it was found that the roof had sufficient structural integrity.

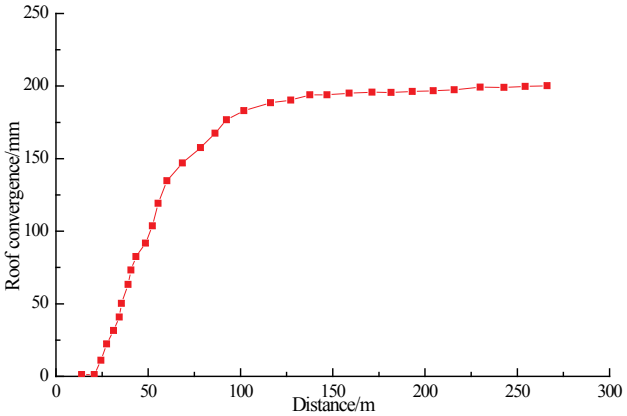

Figure 11 Roof dynamic subsidence on site

6 CONCLUSIONS

(1) By conducting rheological experiments on backfill materials, the relationship between strain and time was obtained. Then, based on these rheological properties, a PTH model was selected. The modelling results presented a good fit to the rheological backfill material data.

(2) Based on the characteristics of the strata movement when using solid backfill mining, the roof and backfill materials were regarded as a thin elastic plate and a viscoelastic foundation respectively to establish the rheological mechanical model of the roof. According to the elastic-viscoelastic correspondence principle, the deflection of the roof on its viscoelastic foundation was obtained.

(3) By combining specific engineering examples, the time-dependent roof subsidence in the 7203W backfill mining panel was acquired. Then, the actual subsidence of the roof was measured, which showed that the theoretical value was similar to that measured. The observations from boreholes drilled into the roof evinced sufficient structural integrity.

Acknowledgements

This research was supported by the Foundation for Innovative Research Groups of the National Natural Science Foundation of China (51421003) and the Fundamental Research Funds for the Central Universities (China University of Mining and Technology) (2014ZDPY02).

7 REFERENCES

[1] Li, M., Zhang J. X., Miao X. X. & Huang, Y. L. (2014). Strata movement under compaction of solid backfill body. *Journal of China University of Mining & Technology, 43*(6), 969-973.

[2] Miao, X. X. (2012). Progress of fully mechanized mining with solid backfilling technology. *Journal of China Coal Society, 37*(18), 1247-1255.

[3] Li, M., Zhang, J. X. & Miao, X. X. (2014). Experimental investigation on compaction properties of solid backfill materials. *Mining Technology, 123*(4), 193-198. https://doi.org/10.1179/1743286314Y.0000000066

[4] Zhang, J. X., Zhang, Q., Sun, Q., Germain, D. & Abro, S. (2015). Surface subsidence control theory and application to backfill coal mining technology. *Environmental Earth Sciences, 74*(2), 1439-1448. https://doi.org/10.1007/s12665-015-4133-0

[5] Junker, M. & Witthaus, H. (2013). Progress in the research and application of coal mining with stowing. *International Journal of Mining Science and Technology, 23*(1), 7-12. https://doi.org/10.1016/j.ijmst.2013.01.002

[6] Ma, Z., Gong, P., Fan, J. Q., Geng, M. M. & Zhang, G. W. (2011). Coupling mechanism of roof and supporting wall in gob-side entry retaining in fully-mechanized mining with gangue backfilling. *Mining Science and Technology (China), 21*(6), 829-833. https://doi.org/10.1016/j.mstc.2011.05.036

[7] Guo, G. L., Feng, W. K., Zha, J. F., Liu, Y. X. & Wang, Q. (2011). Subsidence control and farmland conservation by solid backfilling mining technology. *Transactions of Nonferrous Metals Society of China, 21*(S3), s665-s669. https://doi.org/10.1016/S1003-6326(12)61659-8

[8] Guo, G. L., Zhu, X. J., Zha, J. F. & Wang, Q. (2014). Subsidence prediction method based on equivalent mining height theory for solid backfilling mining. *Transactions of Nonferrous Metals Society of China, 24*(10), 3302-3308. https://doi.org/10.1016/S1003-6326(14)63470-1

[9] Zhang, J. X., Li, J., An, T. L. & Huang, Y. L. (2010). Deformation characteristic of key stratum overburden by raw waste backfilling with fully-mechanized coal mining technology. *Journal of China Coal Society, 35*(3), 357-362.

[10] Li, M., Zhang, J. X., Jiang, H. Q., Huang, Y. L. & Zhang, Q. (2014). A thin plate on elastic foundation model of overlying strata for dense solid backfill mining. *Journal of China Coal Society, 39*(12), 2369-2373.

[11] Huang, Y. L., Zhang, J. X. & Du, J. (2012). Time-dependence of backfilling body in fully mechanized backfilling mining face. *Journal of China University of Mining & Technology, 41*(5), 697-701.

[12] Ju, F., Zhang, J. X. & Zhang, Q. (2012). Vertical transportation system of solid material for backfilling coal mining technology. *International Journal of Mining Science and Technology, 22*(1), 41-45. https://doi.org/10.1016/j.ijmst.2011.07.004

[13] Zhang, Q., Zhang, J. X., Huang, Y. L. & Ju, F. (2012). Backfilling technology and strata behaviors in fully mechanized coal mining working face. *International Journal of Mining Science and Technology, 22*(2), 151-157. https://doi.org/10.1016/j.ijmst.2011.08.003

[14] Miao, X., Ju, F., Huang, Y. L. & Guo, G. L. (2015). New development and prospect of backfilling mining theory and technology. *Journal of China University of Mining & Technology, 44*(3), 391-399.

[15] Li, W. X., Cao, C. Y., Yin, X., Li, J. W., Qi, D. L. & Ren, J. C. (2015). A visco-elastic theoretical model for analysis of dynamic ground subsidence due to deep underground mining. *Applied Mathematical Modelling, 39*(18), 5495-5506. https://doi.org/10.1016/j.apm.2015.01.003

[16] Wang, J. A., Li, D. Z. & Shang, X. C. (2012). Creep failure of roof stratum above mined-out area. *Rock Mechanics and Rock Engineering, 45*(4), 533-546. https://doi.org/10.1007/s00603-011-0216-8

Contact information:

Meng LI
Key Laboratory of Deep Coal Resources Mining,
School of Mines, Ministry of Education of China,
China University of Mining & Technology,
Xuzhou 221116, China
E-mail: cumtmengli@gmail.com

Jixiong ZHANG, corresponding author
Key Laboratory of Deep Coal Resources Mining,
School of Mines, Ministry of Education of China,
China University of Mining & Technology,
Xuzhou 221116, China
E-mail: zjxiong@cumt.edu.cn

Rui GAO
Key Laboratory of Deep Coal Resources Mining,
School of Mines, Ministry of Education of China,
China University of Mining & Technology,
Xuzhou 221116, China
E-mail: papergr@126.com